Secular increase of seasonal predictability for the 20th century

In-Sik Kang,[1] Emilia Kyung Jin,[1] and Kyong-Hee An[1]

Received 6 September 2005; revised 30 November 2005; accepted 9 December 2005; published 19 January 2006.

[1] Seasonal predictability of global surface air temperature for the 100 years of 20th century is examined using the Climate of the 20th Century international project (C20C) AGCM experiment. The C20C experiments reproduce reasonably well the observed warming trend over the globe. The perfect model concept, one simulation being considered as observation, is utilized to examine the changes of seasonal mean predictability for the last 100 years. The global pattern correlations of seasonal mean temperature show clearly the seasonal mean predictability being increased since 1920s. The analysis of the ensemble mean and deviation also shows that the signal to noise ratio is much increased for the recent 30 years, particularly in the tropical and subtropical Pacific. The increase of the seasonal predictability is found to be related to the enhancement of SST variability over the tropical Pacific, which appears to be related to the global warming. **Citation:** Kang, I.-S., E. K. Jin, and K.-H. An (2006), Secular increase of seasonal predictability for the 20th century, *Geophys. Res. Lett.*, *33*, L02703, doi:10.1029/2005GL024499.

1. Introduction

[2] The climate data for 20th century clearly shows global warming trend at the surface and troposphere [*Schlesinger and Mitchell*, 1987; *Lau and Weng*, 1999; *Santer et al.*, 2000; *Intergovernmental Panel on Climate Change*, 2001]. Associated with the global warming, changes of ENSO characteristics, particularly the frequency and amplitude, have been one of important subjects of recent climate research [e.g., *Trenberth and Hoar*, 1996; *An and Wang*, 2000; *Chen et al.*, 2004] due to its extensive impact on the global climate system [e.g., *Rasmusson and Wallace*, 1983; *Kiladis and Diaz*, 1989; *Pan and Oort*, 1990; *Glantz et al.*, 1991]. Analysis of historical observations of sea surface temperature (SST) indicate that El Niño had relatively high amplitude during the period of 1885–1915, ensued by a few decades of relatively low amplitude (1915–1950), and followed by a return to higher amplitudes since about 1960 [*Knutson et al.*, 1997; *Gu and Philander*, 1997; *Wang and Ropelewski*, 1995]. Such changes of ENSO intensity may modulate the global climate circulation anomalies and in turn may change the global predictability, since the predictable signal of atmospheric seasonal mean is considered to arise from the slowing varying boundary conditions at the earth's surface, peculiarly SST anomalies [*Charney and Shukla*, 1981; *Palmer and Anderson*, 1994; *Shukla*, 1998]. Despite of a number of studies on the climatological state of seasonal predictability [*Gates et al.*, 1999; *Shukla et al.*, 2000; *Kang et al.*, 2003a], there has been limited quantitative assessment so far for long-term changes of seasonal predictability, particularly under the decadal modulation of ENSO and/or the global warming.

[3] The signal to noise ratio of seasonal mean is the most relevant parameter for the potential seasonal predictability [*Rowell et al.*, 1995; *Kumar and Hoerling*, 2000]. The signal, which is potentially predictable, is related to atmospheric response to the boundary conditions such as SST and atmospheric composition. On the other hand, the noise is generated internally in the atmosphere and therefore a non-predictable part. It is problematic to separate the signal and noise components in observed data [*Rowell*, 1998], so this kind of study has been carried out by using ensemble AGCM simulations with prescribed SST condition, where all ensemble members are forced by the same SST but started from slightly different atmospheric initial conditions [*Harzallah and Sadourny*, 1995; *Stern and Miyakoda*, 1995; *Kumar and Hoerling*, 2000]. The basic idea of this approach is that the differences among the ensemble members can be used to quantify the random noise due to internal dynamics, whereas the relative similarity between ensemble members can be considered as the atmospheric response to the external forcing.

2. Data and Model

[4] For the present study, a set of 100-year ensemble simulations were performed using a Seoul National University (SNU) AGCM [*Kang et al.*, 2003a] with triangular 42 horizontal resolution (2.8125° latitude by 2.8125 longitude grid) and 20 vertical levels. This experiment is a part of International Climate of the Twentieth Century Project (C20C), which is designed to characterize the climate variability and predictability of the last 100 years through analysis of observational data and ocean-forced atmospheric general circulation models [*Folland et al.*, 2002]. Four member ensemble experiments from January 1897 to November 1998 have performed with different initial conditions. Each simulation was forced according to the C20C experimental protocol using Hadley Centre provides HadISST1.1 SST and sea ice data [*Rayner et al.*, 2003] as lower boundary conditions along with PCMDI vertical ozone distribution and 100-year mean atmospheric CO_2 concentration (321.07 ppm). The data used are the winter (DJF) mean surface air temperature and precipitation.

3. Results

[5] Figures 1a and 1b, respectively, show the linear trends of annual mean surface air temperature, observed and simulated for the 20th century. Comparison of the Figures 1a and 1b indicates that the model mimics the

[1]School of Earth and Environmental Sciences, Seoul National University, Seoul, Korea.

0094-8276/06/2005GL024499$05.00

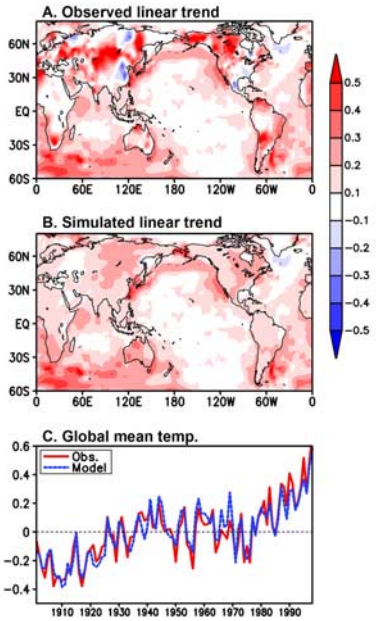

Figure 1. (a) Distribution of linear trend of observed surface air temperature for the 100 years of 1890–1990 and (b) as in Figure 1a except for the simulated linear trend. (c) The time series of global mean temperature anomaly for the observed (Red) and simulated (Blue), respectively.

global distribution of observed warming trend, although the regional details are different, particularly in East Asia and southeast North America, where relatively large cooling trends are observed. This results is coincide with previous studies showing that the AGCM would capture many of the predictable portion under the influence of slowly varying boundary forcing [*Charney and Shukla*, 1981; *Shukla*, 1998]. The simulated global-mean warming trend (0.56°C/100 yr) is close to the observed trend of 0.57°C/100 yr (Figure 1c). For only land area, 0.64°C/100 yr for observed trend and 0.61°C/100 yr for simulated trend. Although not shown here, the model simulates reasonably well the observed characteristics of climatological mean states and interannual variations of seasonal means, as seen in the CLIVAR/AGCM Monsoon intercomparison [*Kang et al.*, 2003a, 2003b].

[6] The potential seasonal predictability is assessed using the ensemble C20C simulations. Here, the potential predictability means the predictability that can be achieved by a AGCM with prescribed observed SSTs and it is measured here in terms of the perfect model correlation. The correlation skill of the perfect model is estimated by considering one of the ensemble members as observation, and the member (observation) is correlated with the ensemble-mean of the other members. Following to the number of ensembles, 4 pattern correlations are averaged for this case. Figure 2 shows the year-to-year variations of the perfect-model global pattern correlations of winter-mean surface air temperature over the continents. The interannual variation of the correlation is shown by gray shading and its nine-year running mean is shown by a black line. Since in the present experiment the surface air temperature follows the prescribed SST over the oceans, the prediction skill shown here is estimated using only the land data. Figure 2 shows the prediction skill has been changed for last 100 years with many time scales with large interannual variations. At first glance, the apparent ascending trend is appeared. The nine-year running mean time series clearly shows that the potential predictability was low for the period of 1914–43 and relatively high during recent several decades. The global pattern correlation of winter-mean precipitation also shows similar results to those seen in Figure 2. In the precipitation case, the low predictability period is for about 30 years of 1920–1949. In the present study, the two 30 year periods of 1914–1943 and 1968–1997 are separated to distinguish the periods of low and high predictability, respectively. The 30 year averaged correlation values of the surface air temperature over global continents are 0.36 and 0.63 for the periods of 1914–43 and 1968–97, respectively.

[7] This big change of predictability is a surprising result and thus checked independently with a different AGCM C20C data to investigate whether this phenomenon is a result from one model or a general feature of AGCMs. The red line in Figure 2 is the nine-year running mean of perfect-model spatial correlation over the land (the counterpart of black line) obtained from the nine member ensemble C20C simulations of NASA/NSIPP model [*Schubert et al.*, 2004]. It has shorter period from 1930 but large ensemble size of 9 with denser resolution of 2.0° latitude by 2.5° longitude grid than SNU GCM used here. Although the NASA data is available only from 1930, the model also clearly shows remarkable increase of potential predictability from 1930 to recent years. Not only the increasing trend of recent year by nine-year running mean, but the interannual predictability of NSIPP is also well matched with that of SNU. Recently, *Nakaegawa et al.* [2004] also showed increase of potential predictability in 500-hPa height since 1950 in their NCEP AGCM 10-member ensemble experiment forced by ERSST.

[8] This striking change of seasonal predictability should be related to the changes of SST variations, since the SST is

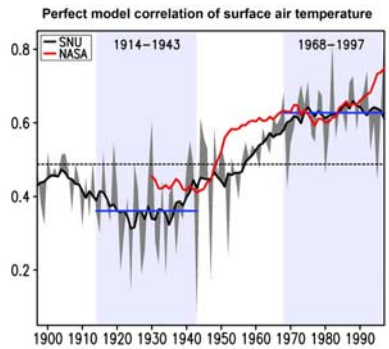

Figure 2. Perfect-model potential predictability of surface air temperature. The potential predictability is measured in terms of the average of the global pattern correlations between one member of the ensemble simulation and the composite of the rest of ensemble members. The gray shaded line indicates correlation value of the winter mean, and black solid line the nine-year running mean of the correlation values, obtained with the SNU AGCM. The red line is the nine-year running mean, obtained with the NASA model.

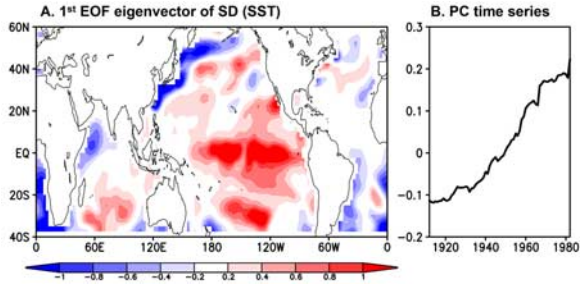

Figure 3. (a) The first EOF eigenvector and (b) associated time series of the 31 year variance of SST over the globe. The 90 year data applied to the EOF is created by moving the center of 31 year window by one year advance for the 90 years.

most dominant external factor to influence the predictability in the present experiment. On the basis of preceding studies showing that ice extents sometimes influence local weather but rarely influence the large-scale flow, we do not allow a separate examination of the influence of sea-ice anomalies [*Walsh*, 1993]. In order to find out the changes of dominant pattern and amplitude of the SST variations for the 20th century, we applied the empirical orthogonal function (EOF) analysis to the SST variance data, created by moving the center of a 31 year window from 1908 to 1987 by one year each. Both in the text and x-axis of Figure 3b, "1913" means the standard deviation of the 31-year averaged SST variance from 1898 to 1928. The first EOF eigenvector and the associated timeseries (Figure 3), which explains 44% of the total variance, indicate that the amplitude of SST variations have been continuously increased from 1920s to recent years, particularly over the ENSO SST region. This result is consistent with previous researches where the ENSO variability in late 20th century appears to be somewhat larger than those in 1920–40 [*Knutson et al.*, 1997; *Gu and Philander*, 1997; *Wang and Ropelewski*, 1995]. Interestingly, the time series shown in Figure 3b is very similar to that of the 9-year running mean of the perfect model global correlation shown in Figure 1, indicating that the variability of tropical Pacific SST indeed influences significantly the seasonal predictability over the globe. The SST standard deviation values averaged for the NINO3 region (5°N–5°S, 90°–150°W) are 0.75°C and 1.09°C for the 1914–43 and 1968–1997 periods, respectively. Such change of ENSO SST amplitude results in the significant change of seasonal potential predictability over the globe.

[9] We also examined how the SST forced and free internal variances of seasonal-mean precipitation have been changed for the 20th century. Precipitation is chosen here as an analysis variable because it is not linearly related to the SST variation over the ocean and thus the analysis can be applied to the global domain (both land and ocean). The forced variance is calculated by using the ensemble means, and the free variances using the deviations of each member from the ensemble mean. As in the above analysis, both variance data for the period of 1912–1982 are obtained by moving the center of 31 year window by one year each for the period. In the text and x-axis of Figure 4d, "1912" means the variance of the 30-year from 1898 to 1927. The four members may not be enough to exactly calculate the forced and free variances, but their characteristic changes can be assessed in the present analysis. The EOF analysis is also applied to the forced and free variance data and to the potential predictability, measured by the ratio of the forced variance to the total variance [*Rowell*, 1998]. The first eigenvectors of the three variables explain about 60% of the total variance of each individual variable (Figures 4a–4c). The time series associated with the three first eigenvectors are all similar (Figure 4d) with an increasing trend. The forced variance of precipitation is pronouncedly increased in the central and western Pacific but not much increased in the tropical eastern Pacific. On the other hand, the change of free variance is more or less randomly distributed and even has a negative sign in many of the tropical regions. As a result, the potential predictability is much enhanced in recent years compared to those in early 20th century over most of the tropics and subtropics. In this study, we do not consider the possible influence of change of the quality in SST data over time on SST variability [*Nakaegawa et al.*, 2004], since we focus on the change of potential seasonal predictability under given history of SST.

[10] The analysis results presented here coincide fairly well with each other. Hence, it can be concluded that the seasonal predictability has been increased significantly with time for the 20th century mainly due to the increase of tropical Pacific SST variability, particularly in the ENSO

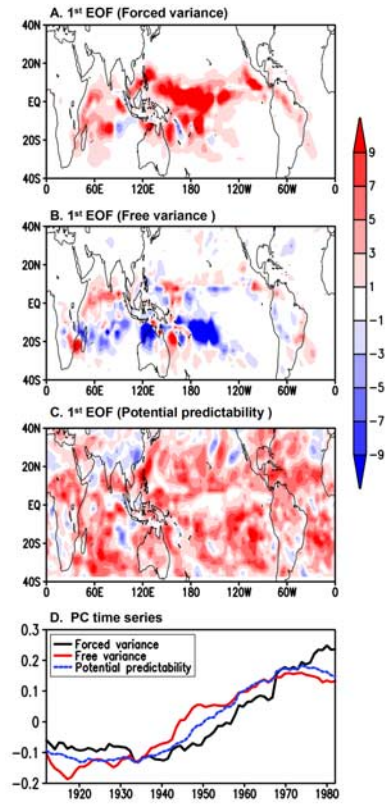

Figure 4. As in Figure 3 except for (a) the forced variance, (b) the free variance, and (c) potential predictability (forced variance divided by total variance) based on the 30 year moving window. (d) The associated time series. Black solid, red solid, and blue dotted lines are for the forced variance, free variances, and the potential predictability, respectively.

region. Recently, there is some evidence that the ENSO amplitude and frequency are influenced by the human-induced global warming [*Meehl and Washington*, 1996; *Trenberth and Hoar*, 1996; *Timmermann et al.*, 1999]. If it is the case, the seasonal mean prediction may be more hopeful for the next century.

[11] **Acknowledgments.** The authors were supported by the Monsoon Research and Seasonal Prediction Projects sponsored by Korea Meteorological Administration and the Eco-technopia 21 project sponsored by Ministry of Environment. We thank the Korean Science and Engineering Foundation for supporting the Climate Environment System Research Center.

References

An, S.-I., and B. Wang (2000), Interdecadal change of the structure of the ENSO mode and its impact on the ENSO frequency, *J. Clim.*, *13*, 2044–2055.

Charney, J. G., and J. Shukla (1981), Predictability of monsoons, in *Monsoon Dynamics*, edited by J. Lighthill and R. P. Pearce, p. 99, Cambridge Univ. Press, New York.

Chen, D., M. A. Cane, A. Kaplan, S. E. Zebiak, and D. J. Huang (2004), Predictability of El Niño over the past 148 years, *Nature*, *428*, 733–736.

Folland, C. K., J. Shukla, J. Kinter, and M. J. Rodwell (2002), C20C: The climate of the twenty century project, *CLIVAR Exch.*, *7*, 37–39.

Gates, W. L., et al. (1999), An overview of the results of the atmospheric model intercomparison project (AMIP1), *Bull. Am. Meteorol. Soc.*, *80*, 29–55.

Glantz, M. H., R. W. Katz, and N. Nicholls (1991), *Teleconnections Linking Worldwide Climate Anomalies*, 535 pp., Cambridge Univ. Press, New York.

Gu, D., and S. G. H. Philander (1997), Interdecadal climate fluctuations that depend on exchanges between the tropics and extratropics, *Science*, *275*, 805–807.

Harzallah, A., and R. Sadourny (1995), Internal versus SST-forced atmospheric variability as simulated by an atmospheric general circulation model, *J. Clim.*, *8*, 474–495.

Intergovernmental Panel on Climate Change (2001), *Climate Change 2001: The Scientific Basis*, edited by J. T. Houghton et al., 881 pp., Cambridge Univ. Press, New York.

Kang, I.-S., et al. (2003a), Intercomparison of atmospheric GCM simulated anomalies associated with the 1997/98 El Nino, *J. Clim.*, *15*, 2791–2805.

Kang, I.-S., et al. (2003b), Intercomparison of the climatological variations of Asian summer monsoon precipitation simulated by 10 GCMs, *Clim. Dyn.*, *19*, 383–395.

Kiladis, G. N., and H. F. Diaz (1989), Global climatic anomalies associated with extremes in the Southern Oscillation, *J. Clim.*, *2*, 1069–1090.

Knutson, T. R., S. Manabe, and D. Gu (1997), Simulated ENSO in a global coupled ocean-atmosphere model: Multidecadal amplitude modulation and CO_2 sensitivity, *J. Clim.*, *10*, 138–161.

Kumar, A., and M. P. Hoerling (2000), Analysis of a conceptual model of seasonal climate variability and implications for seasonal prediction, *Bull. Am. Meteorol. Soc.*, *81*, 255–264.

Lau, K.-M., and H. Weng (1999), Interannual, decadal-interdecadal, and global warming signals in sea surface temperature during 1955–97, *J. Clim.*, *12*, 1257–1267.

Meehl, G. A., and W. M. Washington (1996), El Nino-like climate change in a model with increased atmospheric CO_2 concentrations, *Nature*, *382*, 56–60.

Nakaegawa, T., M. Kanamitsu, and T. M. Smith (2004), Interdecadal trend of prediction skill in an ensemble AMIP-type experiment, *J. Clim.*, *17*, 2881–2889.

Palmer, T. N., and D. L. T. Anderson (1994), The prospects for seasonal forecasting—A review paper, *Q. J. R. Meteorol. Soc.*, *120*, 755–793.

Pan, Y.-H., and A. H. Oort (1990), Correlation analyses between sea surface temperature anomalies in the eastern equatorial Pacific and the world ocean, *Clim. Dyn.*, *4*, 191–205.

Rasmusson, E. M., and J. M. Wallace (1983), Meteorological aspects of the El Nino/Southern Oscillation, *Science*, *222*, 1195–1202.

Rayner, N. A., D. E. Parker, E. B. Horton, C. K. Folland, L. V. Alexander, D. P. Rowell, E. C. Kent, and A. Kaplan (2003), Global analyses of sea surface temperature, sea ice, and night marine air temperature since the late nineteenth century, *J. Geophys. Res.*, *108*(D14), 4407, doi:10.1029/2002JD002670.

Rowell, D. P. (1998), Assessing potential seasonal predictability with and ensemble of multidecadal GCM simulations, *J. Clim.*, *11*, 109–120.

Rowell, D. P., C. K. Folland, K. Maskell, and N. Waed (1995), Variability of summer rainfall over tropical north Africa (1906–92): Observations and modeling, *Q. J. R. Meteorol. Soc.*, *121*, 669–704.

Santer, B. D., et al. (2000), Interpreting differential temperature trends at the surface and in the lower troposphere, *Science*, *287*, 1227–1232.

Schlesinger, M. E., and J. F. B. Mitchell (1987), Climate model projections of the equilibrium climatic response to increased CO_2, *Rev. Geophys.*, *25*, 760–798.

Schubert, S. D., M. J. Suarez, P. J. Pegion, R. D. Koster, and J. T. Bacmeister (2004), Causes of long-term drought in the U.S. Great Plains, *J. Clim.*, *17*, 485–503.

Shukla, J. (1998), Predictability in the midst of chaos: A scientific basis for climate forecasting, *Science*, *282*, 728–731.

Shukla, J., et al. (2000), Dynamical seasonal prediction, *Bull. Am. Meteorol. Soc.*, *81*, 2593–2606.

Stern, W., and K. Miyakoda (1995), The feasibility of seasonal forecasts speculated from multiple GCM simulations, *J. Clim.*, *8*, 1071–1085.

Timmermann, A., M. Latif, A. Bacher, J. Oberhuber, and E. Roeckner (1999), Increased El Nino frequency in a climate model forced by future greenhouse warming, *Nature*, *398*, 694–696.

Trenberth, K., and T. Hoar (1996), The 1990–1995 El Nino-Southern Oscillation event: Longest on record, *Geophys. Res. Lett.*, *23*, 57–60.

Walsh, J. E. (1993), Observational and modelling studies of the influence of sea ice anomalies on atmospheric circulation, in *Prediction of Interannual Climate Variations*, edited by J. Shukla, p. 71, Springer, New York.

Wang, X. L., and C. F. Ropelewski (1995), An assessment of ENSO-scale secular variability, *J. Clim.*, *8*, 1584–1599.

I.-S. Kang, E. K. Jin, and K.-H. An, School of Earth and Environmental Sciences, Seoul National University, Seoul 151-742, Korea. (kang@climate.snu.ac.kr)